

Stability or Instability of a Static Meniscus Appearing in Ribbon Single Crystal Growth from Melt using E.F.G. Method

Andreea V. Cojocaru¹, Adriana Tanasie¹, Stefan Balint^{1*} and Sorina M.D. Laitin²

¹Department of Computer Science, West University of Timisoara, Blvd. V. Parvan 4, 300223 Timisoara, Romania

²Department 13, Victor Babes University of Medicine and Pharmacy Timisoara, Eftimie Murgu Nr.2, 300041 Timisoara

*Corresponding Author

Stefan Balint, Department of Computer Science, West University of Timisoara, Blvd. V. Parvan 4, 300223 Timisoara, Romania.

Submitted: 2025, Apr 18; **Accepted:** 2025, May 05; **Published:** 2025, May 19

Citation: Cojocaru, A. V., Tanasie, A., Balint, S., Laitin, S. M. D. (2025). Stability or Instability of a Static Meniscus Appearing in Ribbon Single Crystal Growth from Melt using E.F.G. Method. *J Sen Net Data Comm*, 5(2), 01-11.

Abstract

This study presents necessary conditions for the existence and sufficient conditions for the stability or instability of the static meniscus (liquid bridge) appearing in the ribbon single crystal growth from the melt, of predetermined sizes, by using the edge-defined-film-fed (EFG) growth method. The cases when the contact angle and the growth angle verify the inequality $0 < \alpha_c < \frac{\pi}{2} - \alpha_g$ or $\frac{\pi}{2} > \alpha_c > \frac{\pi}{2} - \alpha_g$ are treated separately. Experimentally, only static meniscus (liquid bridges) which verifies the necessary condition of existence and the sufficient conditions of stability can be created; static meniscus (liquid bridges) which does not verify both of these conditions, exist only in theory because in reality they collapses. The results of this study is significant for thin ribbon single crystal growth from melt, with prior given macroscopic dimensions, using prior given specific equipment. That is because the obtained inequalities represent limits for what can and cannot be achieved experimentally.

Keywords: Static Stability, Meniscus, Ribbon Growth, Edge-Defined-Film-Fed-Growth

1. Introduction

The basic growth methods available for crystal growth are broadly; growth from the melt, growth from vapor, and growth from solution. Modern engineering does not only need single crystals of arbitrary shapes but also plates-, rod and tube-shaped single crystals, i.e. single crystals of shapes that allow one to use them as final products without additional machining. This problem appears to be solved by profiled- container crystallization as in the case of casting. However, this solution is not always acceptable. Container material needs to satisfy a certain set of requirements: should be neither react with the melt nor be wetted by it, it should be of high-temperature and aggressive-medium resistant, etc. Even if all these requirements are satisfied perfect –single crystal growth is not secured and growing very thin plate-shaped single crystals, to say nothing of shapes that are more complicated, excludes container application completely. The Springer Handbook of Crystal Growth present on 1816 pages the state of the art in crystal growth until the years 2010 [1]. In Chapter 40 pg. 1379-1402 of this book the authors Th. George, St. Balint, L. Braescu presents several mathematical models describing processes, which take place in case of crystal growth from the melt by Bridgman-Stock Barger (BC) and by Edge-Defined-Film-Fed –Growth (EFG) method. For BC growth of cylindrical bar see Figure.1.1 for ribbon (thin plate) growth by EFG method see Figures 1.2 ,1.3.

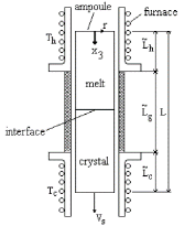


Figure: 1.1 Cylindrical bar

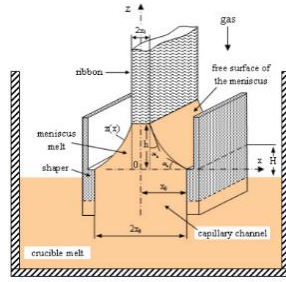


Figure: 1.2 Ribbon, $0 < \alpha_c \leq \frac{\pi}{2} - \alpha_g$.

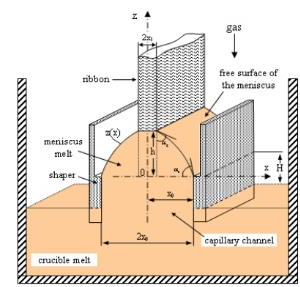


Figure: 1.3 Ribbon, $\frac{\pi}{2} > \alpha_c > \frac{\pi}{2} - \alpha_g$.

In case of the BS method, the melt is encapsulated in a crucible and the crystallization of the melt takes place in conditions of permanent contact between the melt and the crystal with the inner wall of the crucible. A significant advantage of the EFG method in comparison with respect to the BS method is that the crystal is grown without interaction with the crucible, which considerably improves the structural quality of the material: less residual stresses, dislocations, spurious nucleation or twins. In case of EFG method, there is a liquid bridge between the crystal and the shaper (die), called meniscus. The melt is in a crucible, from which it flows through a capillary channel onto the surface of the shaper Figure 1.2. Figure 1.3. Here a liquid bridge is formed between the shaper surface and the crystal. The crystallization takes place on the so “called crystallization front” which is the border line between the upper part of the liquid bridge and the bottom of the crystal. In the second section of this paper a short mathematical description of the real problem is given. Along with the equations, boundary conditions, and initial values defining the model are presented. In the third section in the framework of the mathematical model, predictions are made concerning the stability and instability of convex meniscus. In the fourth section in the framework of the same mathematical model, predictions are made concerning the stability and instability of concave meniscus. These predictions are made analyzing the static stability or instability of meniscus with theoretical tools presented in [2]. In the fifth section we discuss the problem what is wanted and what can be done.

2. Mathematical Description of Meniscus Free Surface

The free surface of the static meniscus, in single crystal growth by EFG method, in hydrostatic approximation is described by the Young-Laplace capillary equation [3,4]:

$$\gamma \times \left(\frac{1}{R_1} + \frac{1}{R_2} \right) = P_a - P_m \quad (2.1)$$

Here: γ is the melt surface tension; $\frac{1}{R_1}, \frac{1}{R_2}$ denote the main normal curvatures of the free surface at an arbitrary point M of the meniscus; P_a is the pressure above the free surface, equal to the pressure of the gas flow introduced in the furnace for release the heat and thereafter is denoted by p_g ($P_a = p_g$). The pressure P_m under the free surface is the sum of the hydrodynamic pressure in the meniscus melt (due to the thermal convection) and the hydrostatic pressure of the melt column equal to $-\rho \times g \times (z + H)$ (see Figure 1.2, Figure 1.3). Here: ρ denotes the melt density; g is the gravity acceleration; z is the coordinate of M with respect to the Oz axis, directed vertically upwards; H denotes the melt column height between the horizontal crucible melt level and the shaper top level. H is positive when the crucible melt level is under the shaper top level and it is negative when the shaper top level is under the crucible melt level.

The pressure difference $P_a - P_m$ across the free surface is $P_a - P_m = p_g - p_m + \rho \times g \times (z + H) = \rho \times g \times z - (p_m - p_g - \rho \times g \times H) = \rho \times g \times z - p$

where $p = (p_m - p_g - \rho \times g \times H)$. In hydrodynamic equilibrium $p_m = 0$ and $p = (-p_g - \rho \times g \times H)$. This pressure difference is constant and it is called the controllable part of the pressure difference $P_a - P_m$.

In hydrostatic approximation the Young-Laplace capillary surface equation can be written as:

$$\gamma \times \left(\frac{1}{R_1} + \frac{1}{R_2} \right) = \rho \times g \times z - p \quad (2.2)$$

Where

$$p = -p_g - \rho \times g \times H \quad (2.3)$$

To calculate the meniscus surface shape and size in hydrostatic approximation is convenient to employ the Young-Laplace equation (2.2) in its differential form:

$$\left[1 + \left(\frac{\partial z}{\partial y}\right)^2\right] \times \frac{\partial^2 z}{\partial x \partial x} - 2 \times \frac{\partial z}{\partial x} \times \frac{\partial z}{\partial y} \times \frac{\partial^2 z}{\partial x \partial y} + \left[1 + \left(\frac{\partial z}{\partial x}\right)^2\right] \times \frac{\partial^2 z}{\partial y \partial y} = \frac{\rho \times g \times z - p}{\gamma} \times \left[1 + \left(\frac{\partial z}{\partial x}\right)^2 + \left(\frac{\partial z}{\partial y}\right)^2\right]^{\frac{3}{2}} \quad (2.4)$$

With respect to the Oxyz, reference frame. (see Figures.1.2,1.3.)

For an Oyz plan symmetric meniscus $\frac{\partial z}{\partial y} = 0$ equation (2.4) become

$$z'' = \frac{\rho \times g \times z - p}{\gamma} \times \sqrt{[1 + z'^2]^3} \quad \text{for } x_1 \leq x \leq x_0 \quad (2.5)$$

where: $x_1 > 0$ is the single crystal ribbon half-thickness and x_0 ($x_0 > x_1$) is the shaper half-thickness.

Equation (2.5) is the Euler equation for the free energy functional $I(z)$ of the melt column

$$I(z) = \int_{x_1}^{x_0} \left\{ \gamma \times [1 + \sqrt{1 + (z')^2}] - \frac{1}{2} \times \rho \times g \times z^2 - p \times z \right\} dx \quad z(x_1) = h, \quad z(x_0) = 0 \quad (2.6)$$

The Euler equation is the first order necessary condition of minimum of the functional (2.6). Namely

$$\frac{d}{dx} \left(\frac{\partial F}{\partial z'} \right) - \left(\frac{\partial F}{\partial z} \right) = 0, \quad F(x, z, z') = \left\{ \gamma \times [1 + \sqrt{1 + (z')^2}] + \frac{1}{2} \times \rho \times g \times z^2 - p \times z \right\} \quad (2.7)$$

As the Young- Laplace equation in hydrostatic approximation (2.5) is a second order differential equation formulation of boundary conditions requires assignment of two boundary conditions; one of the melt crystal interfaces, the second one on the melt and shaper interface. These conditions are: solution $z = z(x)$ of the Eq. (2.5) satisfy the following boundary conditions:

$$\begin{aligned} z'(x_1) &= -\tan\left(\frac{\pi}{2} - \alpha_g\right), \quad z'(x_0) = \tan(\alpha_c), \quad z(x_0) = 0 \quad \text{and} \\ z(x) &\text{is strictly decreasing on } [x_1, x_0] \end{aligned} \quad (2.8)$$

Where α_g is the growth angle, α_c is the contact angle between the meniscus free surface and the edge of the shaper top.

3. Stability or Instability of a Convex Meniscus

A meniscus is convex if $z''(x) > 0$ for $x_1 \leq x \leq x_0$

Remark first that in case of a convex meniscus the function $z'(x)$ is increasing. This means that the angle between the tangent line to meniscus in every point, and the OX axis $\alpha(x) = -\arctan z'(x)$ is decreasing. In particular, it follows that $\alpha(x_1) > \alpha(x_0)$. Since $\alpha(x_1) = \frac{\pi}{2} - \alpha_g$ and $\alpha(x_0) = \alpha_c$ we obtain inequality $\frac{\pi}{2} - \alpha_g > \alpha_c > 0$. (see Figure 1.2)

It should be noted that, the convex meniscus stability (the static one) should be distinguished from the dynamic stability of the crystallization process For statically stable convex meniscus, not only indispensable (necessary) first order but also second order sufficient conditions of functional (2.6) should be satisfied. These second order sufficient conditions for the minimum of functional (2.6) are the Legendre condition and the Jacobi condition [5].

The Legendre condition is

$$\frac{\partial^2 F}{\partial z' \partial z'} > 0 \quad (3.1)$$

Computing $\frac{\partial^2 F}{\partial z' \partial z'}$ we find $\frac{\partial^2 F}{\partial z' \partial z'} = \frac{\gamma}{(1 + (z')^2)^{\frac{3}{2}}} > 0$. Therefore the Legendre condition is satisfied.

The Jacoby condition concern the so-called Jacoby equation:

$$\left[\frac{\partial^2 F}{\partial z \partial z} - \frac{d}{dx} \left(\frac{\partial^2 F}{\partial z \partial z'} \right) \right] \times \eta - \frac{d}{dx} \left[\frac{\partial^2 F}{\partial z' \partial z'} \times \eta' \right] = 0 \quad (3.2)$$

for which a Sturm type upper bound has to be find [5].

In case of the functional (2.6) equation (3.2) become:

$$\frac{d}{dx} \left[\frac{\gamma}{(1+(z')^2)^{\frac{3}{2}}} \times \eta' \right] - g \times \rho \times \eta = 0 \quad (3.3)$$

Remark that for the coefficients of (3.3) the following inequalities hold:

$$\frac{\gamma}{(1+(z')^2)^{\frac{3}{2}}} > \gamma \times (\sin \alpha_g)^3 \quad \text{and} \quad -g \times \rho < 0 \quad (3.4)$$

Hence

$$(\eta' \times \gamma \times (\sin \alpha_g)^3)' = 0 \quad \text{or} \quad \eta'' = 0 \quad (3.5)$$

is a Sturm –type upper bound for (3.3)

Since every non-zero solution of the equation $\eta'' = 0$ vanishes at most once on the interval $x_1 \leq x \leq x_0$ the solution $\eta(x)$ of the initial value problem

$$\frac{d}{dx} \left[\frac{\gamma}{(1+(z')^2)^{\frac{3}{2}}} \times \eta' \right] - g \times \rho \times \eta = 0 \quad \eta(x_1) = 0, \quad \eta'(x_1) = 1 \quad (3.6)$$

has only one zero on the interval $x_1 \leq x \leq x_0$. Hence the stability condition of Jacobi is verified.

This result can be surprising and create the impression that a convex meniscus is stable. In fact, the result is that if a convex meniscus exist, then it is stable. For this reason, in the following, we will establish necessary conditions for the existence of convex meniscus (see Figure.1.2.).

Starting from equations (2.3) and (2.5) it is easy to see that in hydrostatic approximation the pressure difference p verify equalities:

$$p = -p_g - \rho \times g \times H = \gamma \times \alpha' \times \cos \alpha + \rho \times g \times z \quad (3.7)$$

Using $p = \gamma \times \alpha \times \cos \alpha + \rho \times g \times z$, the boundary conditions $\alpha(x_1) = \frac{\pi}{2} - \alpha_g$, $\alpha(x_0) = \alpha_c$, with the Lagrange mean value theorem we obtain that there exists x' in the interval $[x_1, x_2]$ such that

$$p = -\gamma \times \frac{\frac{\pi}{2} - (\alpha_c + \alpha_g)}{x_0 - x_1} \times \cos \alpha(x') + \rho \times g \times z(x') \quad (3.8)$$

Since $\alpha(x)$ is strictly decreasing on the interval $[x_1, x_2]$ the following inequalities hold:

$$\alpha_c \leq \alpha(x') \leq \frac{\pi}{2} - \alpha_g \quad (3.9)$$

$$\sin(\alpha_g) \leq \cos(\alpha(x')) \leq \cos(\alpha_c) \quad (3.10)$$

$$-\rho \times g \times h \leq \rho \times g \times z(x') \leq \rho \times g \times h \quad (3.11)$$

Using equality (3.8) and inequalities (3.9) - (3.11) in hydrostatic approximation, in case of the existence of convex static meniscus, for the pressure difference $p = -p_g - \rho \times g \times H$ the following inequalities hold:

$$-\gamma \times \frac{\frac{\pi}{2} - (\alpha_c + \alpha_g)}{x_0 - x_1} \times \cos(\alpha_c) - \rho \times g \times h \leq -p_g - \rho \times g \times H \leq -\gamma \times \frac{\frac{\pi}{2} - (\alpha_c + \alpha_g)}{x_0 - x_1} \times \sin(\alpha_g) + \rho \times g \times h \quad (3.12)$$

Therefore, in case of convex meniscus the values of the pressure difference $p = -p_g - \rho \times g \times H$ has to be researched in the interval $[L_{left} + L_{right}]$

where:

$$L_{left} = -\gamma \times \frac{\frac{\pi}{2} - (\alpha_c + \alpha_g)}{x_0 - x_1} \times \cos(\alpha_c) - \rho \times g \times h \quad \text{and} \quad L_{right} = -\gamma \times \frac{\frac{\pi}{2} - (\alpha_c + \alpha_g)}{x_0 - x_1} \times \sin(\alpha_g) + \rho \times g \times h \quad (3.13)$$

For

$$p < -\gamma \times \frac{\frac{\pi}{2} - (\alpha_c + \alpha_g)}{x_0 - x_1} \times \cos(\alpha_c) - \rho \times g \times h \quad \text{and for} \quad p > -\gamma \times \frac{\frac{\pi}{2} - (\alpha_c + \alpha_g)}{x_0 - x_1} \times \sin(\alpha_g) + \rho \times g \times h \quad (3.14)$$

convex meniscus like in Figure.1.2 does not exist. These regions of the pressure difference are regions of static instability. A meniscus with p in this region collapse, For p satisfying one of the inequalities (3.14) it is impossible to create experimentally a convex meniscus like in Figure.1.2

Retain that the pressure difference $p = -p_g - \rho \times g \times H$ can be controlled by the gas pressure p_g and the parameter H .

In the following we will illustrate first the existence of convex static meniscus in case of Ge assuming that $h = 0.00019[m]$, $x_1 = 0.0001[m]$, $x_0 = 0.0002[m]$.

In case of Ge $L_{left} = -2302.112493$ [Pa] and $L_{right} = -686.521879$ and a convex meniscus is obtained for $p = -1525[Pa]$. This meniscus is obtained by integrating the initial value problem:

$$z'(x) = -\tan(\alpha(x)) \quad \alpha'(x) = \frac{p - \rho \times g \times x}{\gamma} \times \frac{1}{\cos(\alpha(x))}; \quad z(x_1) = h = 0.00019 \quad \text{and} \quad \alpha(x_1) = 1.361796327. \quad (3.15)$$

The numerical values of ρ , g , γ are: $\rho = 5600[\frac{kg}{m^3}]$, $g = 9.82[\frac{m}{s^2}]$, $\gamma = 0.620[\frac{N}{m}]$, $\alpha(x_1) = \frac{\pi}{2} - \alpha_g = \frac{\pi}{2} - 0.209$ 1.361796327[rad],

$\alpha_g = 0.209[rad]$ is the growth angle in case of Ge growth. The pressure $p = -1525[Pa]$ was found by trial solving (3.15) for different values of p in the range $[-2302, -686]$ [Pa].

The obtained results concerning the meniscus shape $z(x)$ and the variation of $\alpha(x)$ are presented in the next figures:

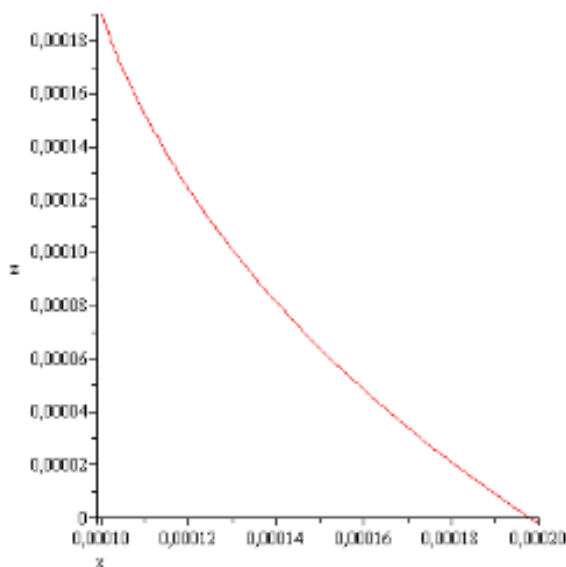


Figure: 3.1 Ge convex meniscus shape for $p = -1525[Pa]$

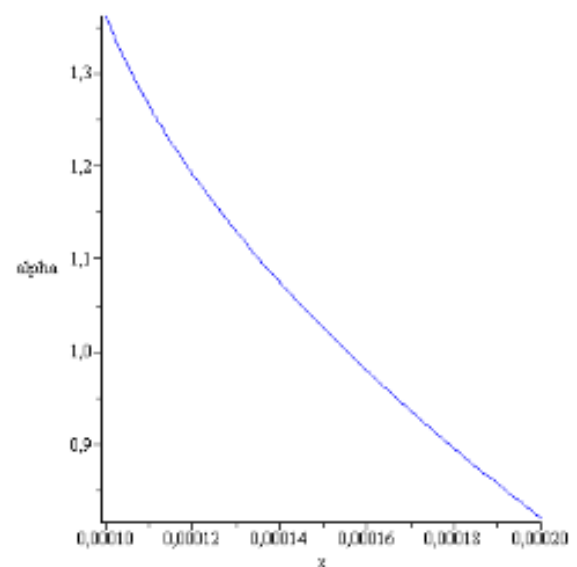


Figure: 3.2 α vrsuse x

For $x = 0.000200000000000000$ we have $\alpha(x) = 0.82070727652608210$ and $z(x) = -0.0000021483692772964195$

According to the above results concerning stability of the static meniscus that obtained here numerically is stable. Can be realized experimentally!

We continue analyzing what happens numerically if $p < -2302.11249[Pa]$ or $> -686.521879[Pa]$.

First, we solve (3.15) for $p = -10000 [Pa]$. The obtained result is presented on Figure.3.3 and Figure 3.4

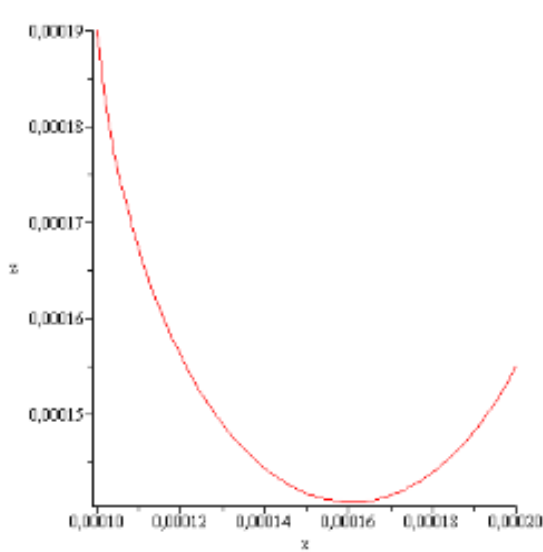


Figure: 3.3 Ge meniscus shape for $p = -10000 [Pa]$.

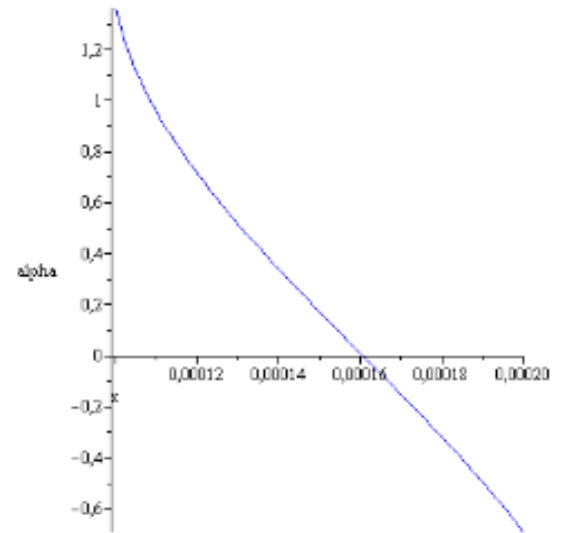


Figure: 3.4 α versus x in case of Ge meniscus

This computation shows that for $p = -10000[Pa]$ the meniscus shape is not convex. The purpose to create a convex meniscus, as in Figure 2.1 is not realizable experimentally!

Now we solve (3.15) for $p = 100[Pa]$. The obtained result is presented on Figure.3.5 and Figure 3.6

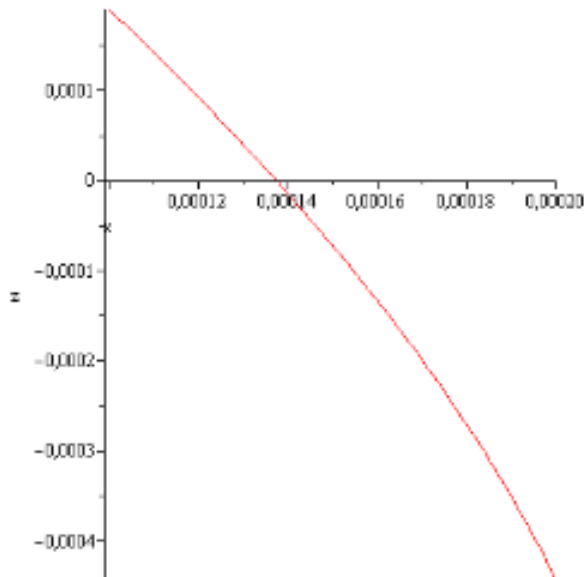


Figure: 3.5 Ge meniscus shape for $p = 100[Pa]$

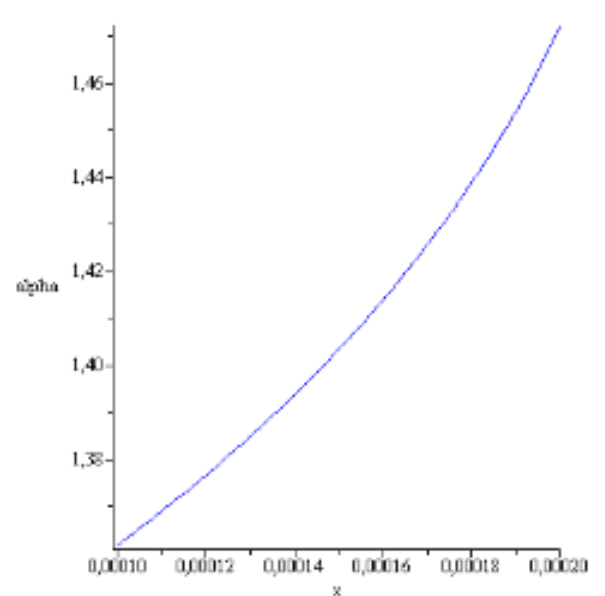


Figure: 3.6 α versus x in case of Ge meniscus

This computation shows that for $p = 100[Pa]$ the meniscus shape is not convex. The purpose to create a convex meniscus, as in Figure.1.2 is not realizable experimentally!

Remember that in hydrostatic approximation $p = -p_g - \rho \times g \times H$. This relation can be used for the control of p via p_g and H .

For example if $p = -1525[Pa]$ then $-1525[Pa] = -p_g - \rho \times g \times H$ and for a given gas pressure p_g we can find, namely $H = \frac{1525 - p_g}{\rho \times g}$. For instance if $p_g = 200[Pa]$ we have $H = \frac{1325}{\rho \times g} = 0.02411897481[m]$. This means that the crucible melt level is under the shaper top level with $0.02411897481[m]$.

If $p = -10000[Pa]$ and $p_g = 200[Pa]$ then $H = \frac{10000 - p_g}{\rho \times g} = \frac{9980}{\rho \times g} = 0.1816659385[m]$. This means that the crucible melt level is under the shaper top level with $0.00182029998[m]$.

This means that the shaper top level is under the crucible melt level with.

4. Stability or Instability of Concave Meniscus

A meniscus is concave if $z''(x) < 0$ for $x_1 \leq x \leq x_0$

Remark that in case of a concave meniscus the function $z'(x)$ is decreasing. Therefore, the angle between the tangent line to meniscus in every point, and the OX axis $\alpha(x) = -\arctan z'(x)$ is increasing. In particular, it follows that $\alpha(x_1) < \alpha(x_0)$. Since $\alpha(x_1) = \frac{\pi}{2} - \alpha_g$ and $\alpha(x_0) = \alpha_c$ we obtain inequality $0 < \frac{\pi}{2} - \alpha_g < \alpha_c$. (see Figure 1.3.)

It should be noted that, the concave meniscus stability (the static one) should be distinguished from the dynamic stability of the crystallization process. For statically stable concave meniscus, not only indispensable (necessary) first order but also second order sufficient conditions of functional (2.6) should be satisfied. These second order sufficient conditions for the minimum of functional (2.6) are the Legendre condition and the Jacobi condition [5]. Since the functional is the same as in convex meniscus case the Legendre condition and the Jacobi condition are the same as in the case of convex meniscus i.e.

$$\frac{\partial^2 F}{\partial z' \partial z'} = \frac{\gamma}{(1+(z')^2)^{\frac{3}{2}}} > 0 \quad (4.1)$$

$$\frac{d}{dx} \left[\frac{\gamma}{(1+(z')^2)^{\frac{3}{2}}} \times \eta' \right] - g \times \rho \times \eta = 0 \quad (4.2)$$

Only the evaluation of coefficients of the equation (4.2) change, and in concave case is given by:

$$\frac{\gamma}{(1+(z')^2)^{\frac{3}{2}}} > \gamma \times (\cos \alpha_c)^3 \text{ and } -g \times \rho < 0. \quad (4.3)$$

Hence

$$(\eta' \times \gamma \times (\cos \alpha_c)^3)' = 0 \quad \text{or} \quad \eta'' = 0 \quad (4.4)$$

is a Sturm-type upper bound for (4.2)

Since every non-zero solution of the equation $\eta'' = 0$ vanishes at most once on the interval $x_1 \leq x \leq x_0$ the solution $\eta(x)$ of the initial value problem

$$\frac{d}{dx} \left[\frac{\gamma}{(1+(z')^2)^{\frac{3}{2}}} \times \eta' \right] - g \times \rho \times \eta = 0 \quad \eta(x_1) = 0, \quad \eta'(x_1) = 1 \quad (4.5)$$

has only one zero on the interval $x_1 \leq x \leq x_0$. Hence the stability condition of Jacobi is verified.

This result can be surprising and create the impression that a concave meniscus is stable. In fact, the result is that if a concave meniscus exist, then it is stable. For this reason, in the following, we will establish necessary conditions for the existence of concave meniscus (see Figure.1.3.)

Starting from equations (2.3) and (2.5) it is easy to see that in hydrostatic approximation the pressure difference p verify equalities:

$$p = -p_g - \rho \times g \times H = \gamma \times \alpha' \times \cos \alpha + \rho \times g \times z \quad (4.6)$$

Using $p = \gamma \times \alpha' \times \cos \alpha + \rho \times g \times z$, the boundary conditions $\alpha(x_1) = \frac{\pi}{2} - \alpha_g$, $\alpha(x_0) = \alpha_c$, with the Lagrange mean value theorem

we obtain that there exists x' in the interval $[x_1, x_2]$ such that

$$p = -\gamma \times \frac{\frac{\pi}{2} - (\alpha_c + \alpha_g)}{x_0 - x_1} \times \cos \alpha(x') + \rho \times g \times z(x') \quad (4.7)$$

Since $\alpha(x)$ is strictly increasing on the interval $[x_1, x_2]$ the following inequalities hold:

$$\frac{\pi}{2} - \alpha_g \leq \alpha(x') \leq \alpha_c \quad (4.8)$$

$$\cos(\alpha_c) \leq \cos(\alpha(x')) \leq \sin(\alpha_g) \quad (4.9)$$

$$-\rho \times g \times h \leq \rho \times g \times z(x') \leq \rho \times g \times h \quad (4.10)$$

Using equality (4.7) and inequalities (4.8) -(4.10) in hydrostatic approximation, in case of the existence of concave static meniscus, for the pressure difference $p = -p_g - \rho \times g \times H$ the following inequalities hold:

$$-\gamma \times \frac{\frac{\pi}{2} - (\alpha_c + \alpha_g)}{x_0 - x_1} \times \cos(\alpha_c) - \rho \times g \times h \leq -p_g - \rho \times g \times H \leq -\gamma \times \frac{\frac{\pi}{2} - (\alpha_c + \alpha_g)}{x_0 - x_1} \times \sin(\alpha_g) + \rho \times g \times h \quad (4.11)$$

Therefore, in case of concave meniscus the values of the pressure difference $p = -p_g - \rho \times g \times H$ has to be researched in the interval $[L_{left}, L_{right}]$ where:

$$L_{left} = -\gamma \times \frac{\frac{\pi}{2} - (\alpha_c + \alpha_g)}{x_0 - x_1} \times \cos(\alpha_c) - \rho \times g \times h, \quad L_{right} = -\gamma \times \frac{\frac{\pi}{2} - (\alpha_c + \alpha_g)}{x_0 - x_1} \times \sin(\alpha_g) + \rho \times g \times h \quad (4.12)$$

$$\text{for } p < -\gamma \times \frac{\frac{\pi}{2} - (\alpha_c + \alpha_g)}{x_0 - x_1} \times \cos(\alpha_c) - \rho \times g \times h \quad \text{and} \quad \text{for } p > -\gamma \times \frac{\frac{\pi}{2} - (\alpha_c + \alpha_g)}{x_0 - x_1} \times \sin(\alpha_g) + \rho \times g \times h \quad (4.13)$$

concave meniscus like in Figure.1.3 does not exist. These regions of the pressure difference are regions of static instability. A meniscus with p in this region collapse. For p satisfying one of the inequalities (4.13) it is impossible to create experimentally a concave meniscus like in Figure.1.3.

Retain that the pressure difference $p = -p_g - \rho \times g \times H$ can be controlled by the gas pressure p_g and the parameter H .

In the following we will illustrate first, the existence of concave static meniscus in case of Ge assuming that $h = 0.00019[m]$, $x_1 = 0.0001[m]$, $x_0 = 0.0002[m]$ and $\alpha_c = 1.4[rad]$. This value of the contact angle can be realized by choosing an appropriate material for shaper.

In case of Germanium $L_{left} = 29.821049[Pa]$ and $L_{right} = 59.582547[Pa]$. It turns that integrating the initial value problem :

$$z'(x) = -\tan(\alpha(x)) \quad \alpha'(x) = \frac{p - \rho \times g \times x}{\gamma} \times \frac{1}{\cos(\alpha(x))} ; \quad z(x_1) = h = 0.00019 \quad \text{and} \quad \alpha(x_1) = 1.361796327 \quad (4.14)$$

the range of pressure difference values of $p \in [29.821049, 59.582547]$ there is no value of p for which concave meniscus exist. A typical solution of (4.14) for is represented in the next figures,

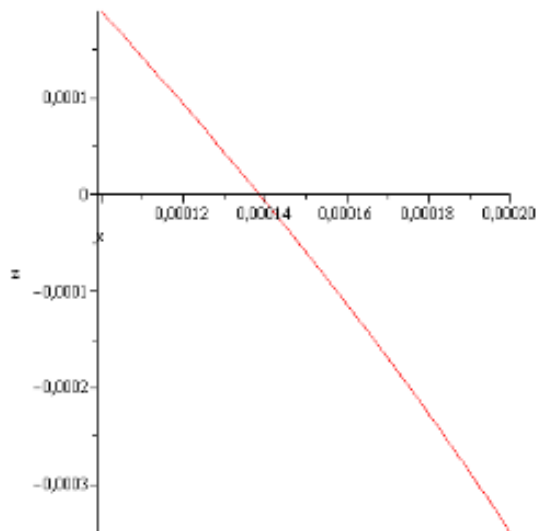


Figure: 4.1 $z(x)$ for $p = 59(Pa)$, $h = 0.00019$

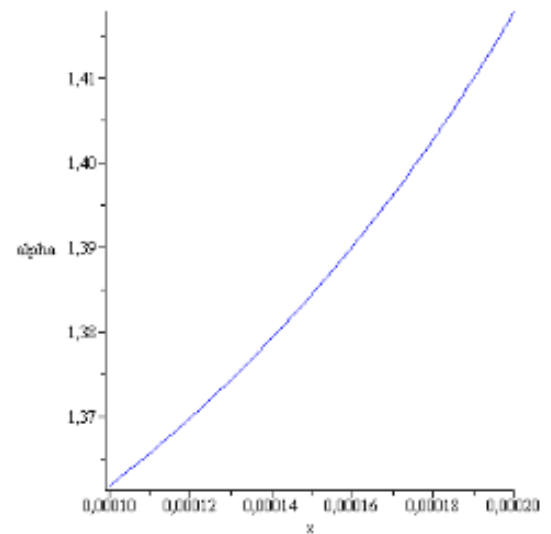


Figure: 4.2 $\alpha(x)$ for $p = 59(Pa)$, $h = 0.00019$

The computed figures show that none of the conditions $z(x_0) = 0[m]$, $\alpha(x_0) = 1.4[Pa]$ is fulfilled. Therefore for $p \in [29.821049, 59.582547][Pa]$ with the prior giving data a concave meniscus like on Figure.1.3. can not be created. Since for $p < 29.821049$ and $p > 59.582547$ concave meniscus like in Figure.1.3. does not exist (see (4.13)) it follows that for the above prior given data concave meniscus can not be created experimentally.

In the same time Figure.4.1. and Figure.4.2. suggest that increasing the level of the crystallization front h creation of a concave meniscus like in Figure.1.3. would be possible. In order to verify the true value of this impression we assume that $h = 2 \times 10^{-3}[m]$ and we compute the corresponding range $[L_{left}, L_{right}]$. We find $[L_{left}, L_{right}] = [-69.613111, 159.016207][Pa]$. This range is larger than that obtained for $h = 0.00019[m]$. Integrating the initial value problem :

$$z'(x) = -\tan(\alpha(x)), \quad \alpha'(x) = \frac{p - \rho \times g \times x}{\gamma} \times \frac{1}{\cos(\alpha(x))}; \quad z(x_1) = h = 2 \times 10^{-3}[m] \text{ and } \alpha(x_1) = 1.361796327[rad] \quad (4.15)$$

for $p \in [-69.613111, 159.016207][Pa]$ the following result is found: there exist a concave meniscus for $p = 141[Pa]$.

The meniscus $z(x)$ and the angle $\alpha(x)$ are represented in the next figures:

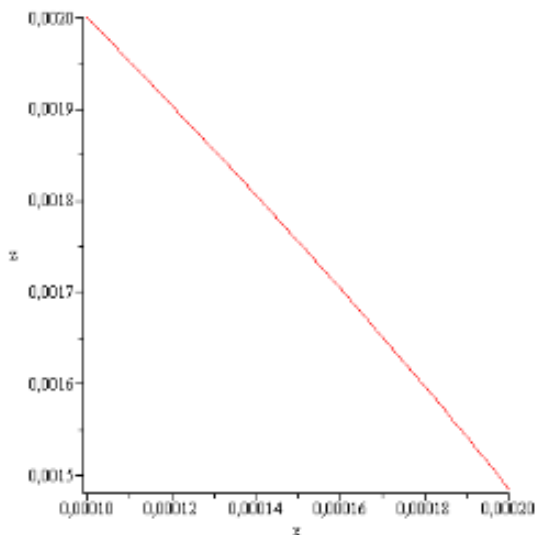


Figure: 4.3 $z(x)$ for $p = 141(Pa)$, $h = 2 \times 10^{-3}[m]$

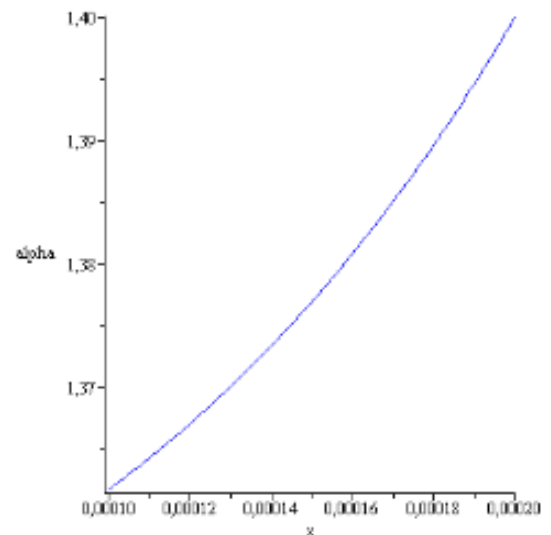


Figure: 4.4 $\alpha(x)$ for, $h = 2 \times 10^{-3}[m]$

This meniscus exist, it is stable and can be created experimentally.

For $p < -69.313111[Pa]$ and $p < -159.0.16207[Pa]$ concave static menisc does not exit. Therefore can not be created experimentally.

A meniscus $z(x)$ and $\alpha(x)$ obtained for $p = -71[Pa]$ are presented in the next figures:

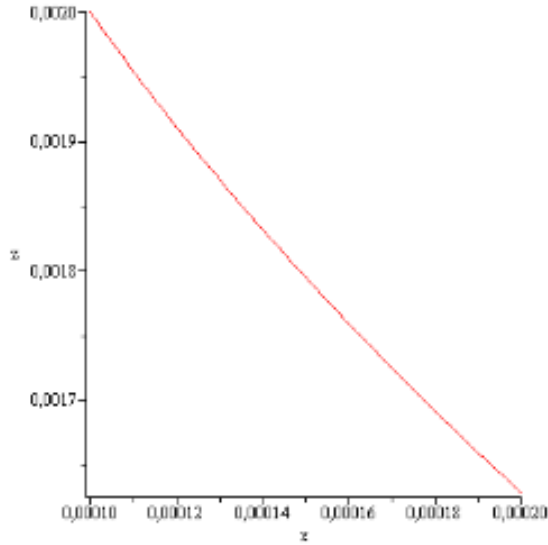


Figure: 4.5 $z(x)$ for $p = -71[Pa]$, $h = 2 \times 10^{-3}[m]$

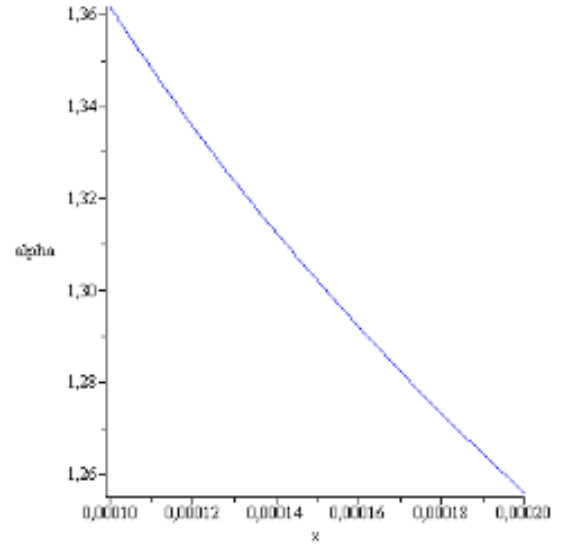


Figure: 4.6 $\alpha(x)$ for, $h = 2 \times 10^{-3}[m]$

A meniscus shape $z(x)$ and $\alpha(x)$ obtained for $p = 161[Pa]$ and $h = 2 \times 10^{-3}[m]$ are represented in the next figures:

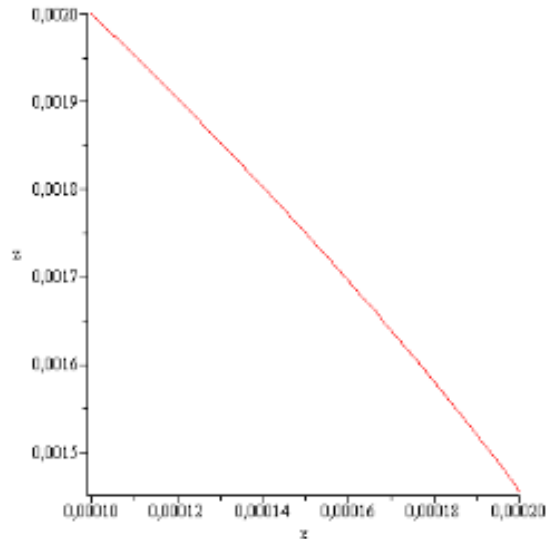


Figure: 4.7 $z(x)$ for $p = 161[Pa]$, $h = 2 \times 10^{-3}[m]$

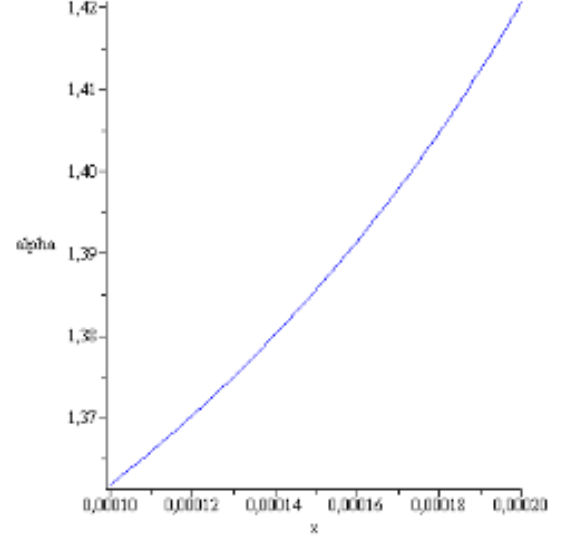


Figure: 4.8 $\alpha(x)$ for, $h = 2 \times 10^{-3}[m]$

Note that experimentally the increase of the crystallization front h from $h = 0.00019[m]$ to $h = 2 \times 10^{-3}$ imply modification of the thermal field.

Remember that in hydrostatic approximation $p = -p_g - \rho \times g \times H$. This relation can be used for the control of p via p_g and H .

For example if $p = 141[Pa] = -p_g - \rho \times g \times H$ then and for a given gas pressure p_g we can find H , namely $H = \frac{141 - p_g}{\rho \times g}$. For instance if $p_g = 100[Pa]$ we have $H = \frac{41}{\rho \times g} = 0.0007463229940[m]$. This means that the crucible melt level is under the shaper top level with $0.0007463229940[m]$.

If $p = -71[Pa]$ and $p_g = 200[Pa]$ then $H = \frac{-271}{\rho \times g} = -0.00493301295[m]$

This means that the shaper top level is under the crucible melt level with $-0.00493301295[m]$.

If $p = 161[Pa]$ and $p_g = 200[Pa]$ then $H = \frac{161-200}{\rho \times g} = \frac{-39}{\rho \times g} = -0.000709916994[m]$. This means that the shaper top level is under the crucible melt level with $-0.000709916994[m]$.

5. Results

Necessary conditions for the existence and sufficient conditions for the stability or instability of the static meniscus (liquid bridge) appearing in the ribbon single crystal growth from the melt, of predetermined sizes, by using the edge-defined-film-fed (EFG) growth method, are presented. Theoretical results are illustrated numerically in case of Germanium ribbon growth.

6. Comments and Conclusions

The main novelty in this article consists in the obtained inequalities. These represent limits for what can and cannot be achieved. Experimentally, only stable static liquid bridges can be created if they exist theoretically. Unstable static liquid bridges could exist just in theory; in reality, they collapse; therefore, they are not appropriate for crystal growth [6,7].

Authors contribution: The authors contributed equally to the realization of this work. All authors have read and agreed to the published version of the manuscript.

Funding: This research did not receive any specific grant from funding agencies in the public, commercial or not-for-profit sectors.

Data Availability Statement: The original contributions presented in the study are included in the article; further inquiries can be directed to the corresponding author.

Conflicts of Interest: The authors declare no conflicts of interest.

References

1. Springer Handbook of Crystal Growth; ISBN:978-3-540-74761-1.
2. Cojocaru, A. V., & Balint, S. (2024). Stability or Instability of a Static Liquid Bridge Appearing in Shaped Crystal Growth from Melt via the Pulling-Down Method. *Fluids*, 9(8), 176.
3. Finn, R. (2012). *Equilibrium capillary surfaces* (Vol. 284). Springer Science & Business Media.
4. V. A. Tatarchenko. (1993) Shaped Crystal Growth, Kluwer Academic Publishers, Dordrecht, The Netherlands.
5. Hartman, P. (2002). *Ordinary differential equations*. Society for Industrial and Applied Mathematics.
6. Balint, S., Balint, A. M., & Szabo, R. (2010). Nonlinear boundary value problem for concave capillary surfaces occurring in single crystal ribbon growth from the melt. *Nonlinear Studies*, 17(1), 65-76.
7. Balint, S., & Balint, A. M. (2008). Nonlinear Boundary Value Problem for Concave Capillary Surfaces Occurring in Single Crystal Rod Growth from the Melt. *Journal of Inequalities and Applications*, 2008, 1-13.

Copyright: ©2025 Stefan Balint, et al. This is an open-access article distributed under the terms of the Creative Commons Attribution License, which permits unrestricted use, distribution, and reproduction in any medium, provided the original author and source are credited.